



1 Article

2 Insight into the self-assembling properties of 3 peptergents: a molecular dynamics simulation study

4 Jean-Marc Crowet ¹, Mehmet Nail Nasir ¹, Nicolas Dony ¹, Antoine Deschamps ², Vincent
5 Stroobant ³, Pierre Morsomme ², Magali Deleu ¹, Patrice Soumillion ², Laurence Lins ^{1,*}

6 ¹ Laboratoire de Biophysique Moléculaire aux Interfaces, Gembloux Agro-Bio Tech, University of Liège,
7 Passage des déportés 2, 5030 Gembloux, Belgium; jmcrowet@ulg.ac.be (J.M.C.); mn.nasir@ulg.ac.be
8 (M.N.N.); n.dony@ulg.ac.be (N.D.); Magali.Deleu@ulg.ac.be (M.D.); l.lins@ulg.ac.be (L.L.)

9 ² Institut des Sciences de la Vie, Université catholique de Louvain, 4-5 Place Croix du Sud, 1348 Louvain-la-
10 Neuve, Belgium; antoine.deschamps@outlook.com (A.D.); pierre.morsomme@uclouvain.be (P.M.);
11 patrice.soumillion@uclouvain.be (P.S.)

12 ³ Ludwig Institute for Cancer Research, de Duve Institute and Université Catholique de Louvain, 75 Avenue
13 Hippocrate, 1200 Brussels, Belgium; vincent.stroobant@bru.licr.org (V.S.)

14 * Correspondence: l.lins@uliege.be; Tel.: +32-81-622644

15 Academic Editor:

16 Received: ; Accepted: ; Published:

17 **Abstract:** By manipulating the various physico-chemical properties of amino acids, design of
18 peptides with specific self-assembling properties has been emerging since more than a decade. In
19 this context, short peptides possessing detergent properties (so-called “peptergents”) have been
20 developed to self-assemble into well-ordered nanostructures that can stabilize membrane proteins
21 for crystallization. In this study, the peptide with “peptergency” properties, called ADA8
22 extensively described by Tao *et al.*, is studied by molecular dynamic simulations for its self-
23 assembling properties in different conditions. In water, it spontaneously form beta sheets with a β
24 barrel-like structure. We next simulated the interaction of this peptide with a membrane protein,
25 the bacteriorhodopsin, in the presence or absence of a micelle of dodecylphosphocholine.
26 According to the literature, the peptergent ADA8 is thought to generate a belt of β structures
27 around the hydrophobic helical domain that could help stabilize purified membrane proteins.
28 Molecular dynamic simulations are here used to image this mechanism and to provide further
29 molecular details for the replacement of detergent molecules around the protein. In addition, we
30 generalized this behavior by designing an amphipathic peptide with beta propensity, called
31 ABZ12. Both peptides are able to surround the membrane protein and displace surfactant
32 molecules. To our best knowledge, this is the first molecular mechanism proposed for
33 “peptergency”.

34 **Keywords:** peptide; self-assembly; molecular dynamic simulations; peptergent

35

36 1. Introduction

37 By manipulating the various physico-chemical properties of amino acids, the design of
38 peptides with specific self-assembling properties has been emerging for some years [1]. Due to their
39 biocompatibility and chemical diversity, peptides are an attractive platform for the design of
40 various nanostructures, such as nanotubes, vesicles, fibers, micelles or rod-coil structures, that have
41 potential applications in drug delivery, tissue engineering or surfactants [2,3]. Depending on the
42 sequence and environment, peptides can self-assemble into ordered structures constrained by non-
43 covalent interactions, such as electrostatic interactions, hydrophobic interactions, van der Waals
44 interactions, hydrogen bonds and π -stacking. Particularly, amphiphilic peptides have shown their
45 ability to self-assemble into a range of nanostructures [3] and behave in some respects like

46 conventional amphiphilic molecules such as surfactants, detergents and lipids. Amphiphaticity can
47 arise either from peptides containing polar and nonpolar residues distributed regularly along the
48 peptide [4] or from alkyl chains linked to a hydrophilic peptide.

49 In that way, short peptides possessing detergent properties (so-called “peptergents”) have
50 been developed in the last decade to self-assemble into well-ordered nanostructures that can
51 stabilize membrane proteins for crystallization [5]. Three main classes are described in the
52 literature: amphiphathic helical peptides [6], lipopeptides [7–9] and short lipid-like peptides [10–12].
53 From a conformational point of view, some of these peptides can adopt α helical or extended β
54 sheet structures during their self-assembly. Recently, the Qinghai Zhang’s group engineered a β -
55 sheet peptide able to self-assemble and to sequester integral membrane proteins (IMPs) [13]. The
56 peptide is amphiphathic, alternating hydrophobic and hydrophilic residues. It is also methylated at
57 some amino groups and is grafted with two alkyl chains. It is proposed that the peptide is able to
58 associate with IMPs in a β barrel-like configuration.

59 There are many detergents available for the solubilization and crystallization of membrane
60 proteins [14]. However, these detergents need to stabilize the native structure of the protein to
61 maintain its function and avoid aggregation. Finding the optimal detergents for the protein studied
62 requires wide screening and depends on the application [12]. New ones are required, and some
63 peptergents have shown better stabilizing properties than commonly used alkyl chain surfactants
64 [15]. Even though experimental evidence is available concerning the relative efficacy of peptergents
65 in solubilizing and stabilizing IMPs [10,11,13,16], little is known about the molecular mechanisms
66 involved in their interactions with proteins.

67 In this work, we studied the self-assembling properties of a known peptide called ADA8 [13]
68 (Fig. 1a) using molecular dynamic (MD) simulations. In water, this peptide is able to self-assemble
69 as a beta barrel-like structure. In the presence of an integral membrane protein, the peptide forms a
70 beta belt around the protein with and without surfactant molecules. To the best of our knowledge,
71 this is the first time that a molecular mechanism is proposed by MD for “peptergency”. Our
72 calculation approach should further serve as a predicting tool for the design of beta peptergent with
73 diverse amphiphathic properties, as suggested for a *de novo* designed peptide, ABZ12.

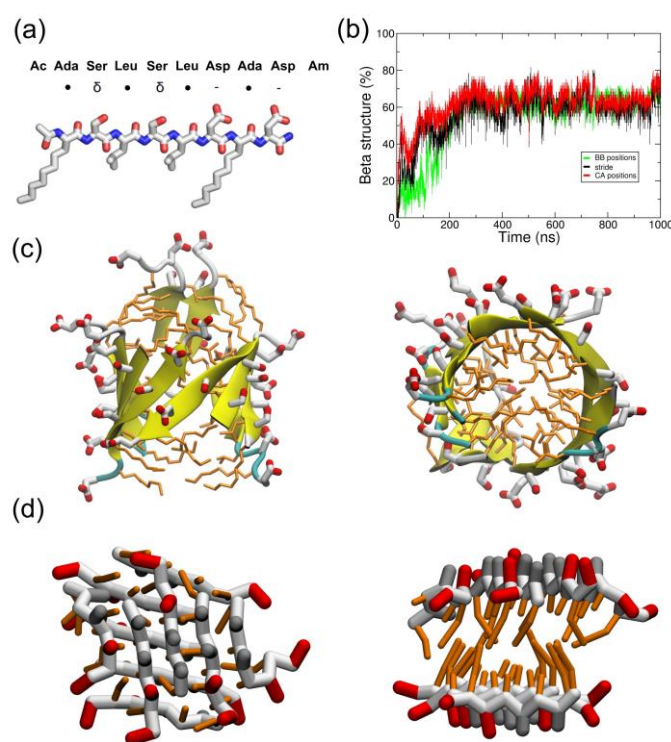
74 2. Results

75 2.1. Simulations in water

76 Ten ADA8 peptides were simulated in water in atomistic (AT) (1 μ s) and coarse grained (CG)
77 (10 μ s) representations to follow their self-assembly (Fig. 1). The black curve of Fig. 1b shows a
78 rapid increase in the beta structure during AT simulations in water and the beta sheets formed can
79 be seen in Fig. 1c and Fig. S1a. These structures are similar to beta barrels with the peptide adopting
80 amphiphilic beta strand conformations with the hydrophobic residues facing the inside of the
81 barrel. The strands can be parallel or anti-parallel. The self-assembly has also been simulated in a
82 CG representation since longer time scales can be achieved. At the end of the CG simulation, we
83 observed two amphiphilic beta sheets facing each other, with the hydrophobic residues buried
84 between the sheets. Polar interactions between sidechains as well as backbone interactions between
85 the strands are also noticed. To estimate the formation of beta structures, a parameter based on $C\alpha$
86 or backbone beads positions has been used (see Methods). As observed in AT simulations, the
87 peptides are able to adopt a beta conformation along the simulation, as assessed by the green curve
88 in Fig. 1b and the molecular assembly in Fig. 1d and Fig. S1b. Though the beta sheet twist observed
89 in atomistic simulations is not reproduced by the CG model and leads to the formation of two
90 facing beta sheets instead of a beta barrel. It is worth noting that the MARTINI force field is, in
91 principle, not designed to sample native conformations [17], especially for beta sheet structures,
92 since there is no hydrogen bond representation. In the literature, several fibril-forming peptides
93 have been studied using MARTINI [18,19], such as the aggregation of the Apo C-II amyloid peptide
94 or the assembly of the protofibrils of amylin. However, beta sheet formation was not observed for
95 the Apo C-II peptide, and the beta conformation of amylin protofibrils was restrained before
96 elongation could occur. Nevertheless, Seo *et al.* have observed beta sheet formation with MARTINI,

97 but they have modified the backbone potentials to reproduce structural properties derived from
 98 atomistic simulations [20]. Here, we observed the appearance of beta sheets without any
 99 modification of the force field; this is mainly due to the beta amphipathic nature of the ADA8
 100 peptide. Some differences between CG and AT beta sheets were nevertheless observed. CG strands
 101 in beta sheets are shifted by one residue compared to atomistic beta sheets (Fig. 1d). In the latter,
 102 the relative positions of the beta strands are defined by hydrogen bonding and the side chains on
 103 both sheet sides align. In contrast, in CG, the attraction comes from the backbone (BB) beads, and
 104 the shifted position minimizes the overall BB bead distance between strands. The question of the
 105 backbone representation in MARTINI was discussed by Marrink *et al.* in 2013; a perspective
 106 evolution of the force field would be to add charged beads to the backbone in order to reproduce
 107 the structural preferences of proteins [21].

108 To assess the stability of the beta structure formed, the structure represented on Fig. 1d has
 109 been transformed to an atomistic resolution and further simulated for 100 ns. This simulation
 110 shows a rapid reorganization of the beta sheets to form beta barrel (Fig. S2). Globally, for all the
 111 simulations, the peptide are able to form beta structures, which agrees with the literature [13].
 112

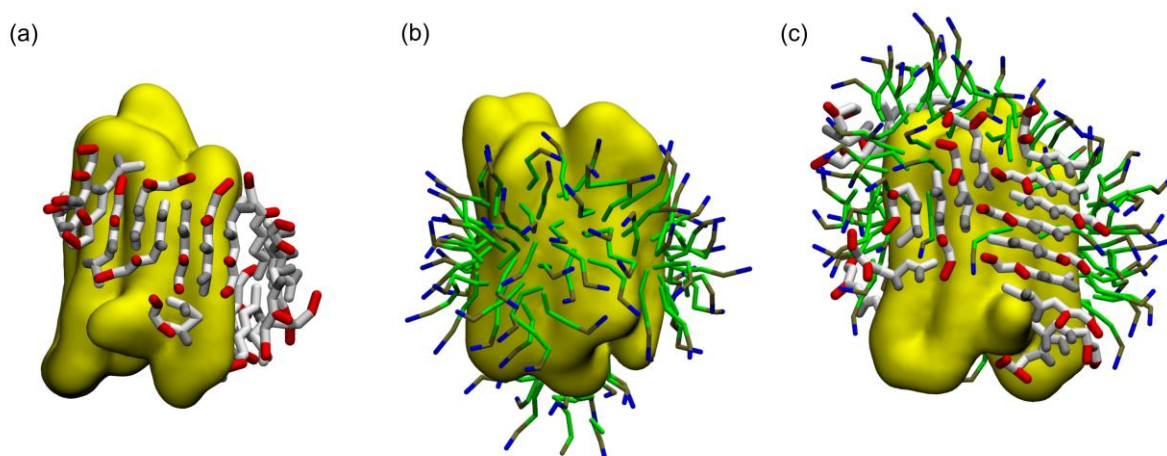


113 **Figure 1. ADA8 peptides structure in water.** (a) Representation of the ADA8 peptide. •, δ and -
 114 represent hydrophobic, polar and negatively charged residues, respectively. (b) Percentage of beta
 115 conformation. The structure is assigned by Stride in AT (black) and by using the following
 116 parameter in CG : a dihedral angle greater than 100° for four following CA atoms and two other
 117 following CA atoms within 6 Å. The red and green curves correspond to this parameter for AT and
 118 CG simulations. Conformations at the end of simulations in atomistic and coarse grained
 119 representations are in panels (c) and (d), respectively; the right panels are an upper view of the left
 120 panels. AT beta sheets are in yellow in the AT representations. Polar, negatively charged and
 121 hydrophobic CG residues are represented in gray, red and orange, respectively.

122 2.2. Coarse grained simulation of the ADA8 peptide in the presence of a membrane protein

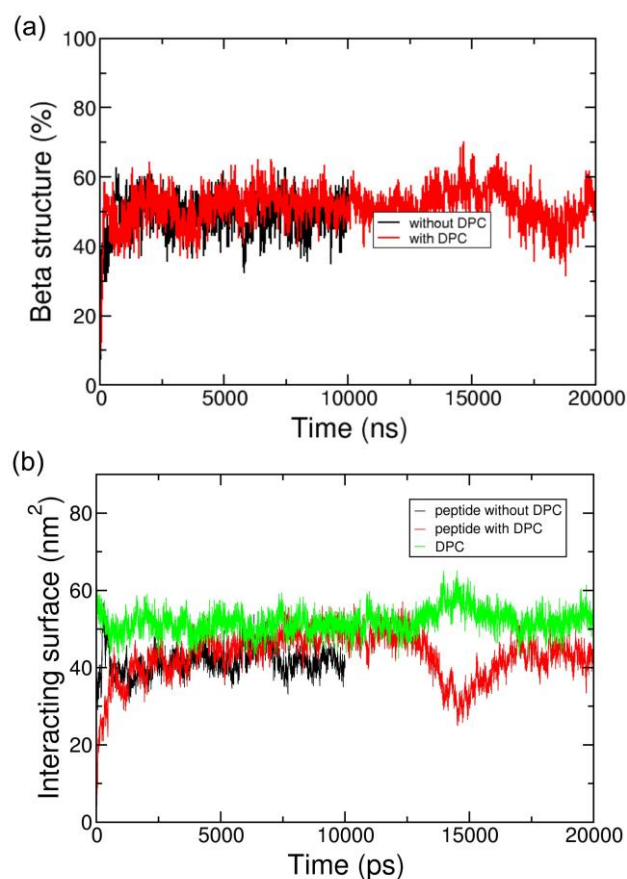
123 ADA8 was shown by Tao *et al.* to be a very efficient peptergent and to solubilize membrane
 124 proteins such as rhodopsin [13]. Thus, we chose an IMP with a known and well-characterized 3D
 125 structure, bacteriorhodopsin (BRD). Twenty peptides were simulated in water in the presence of
 126 one BRD protein over 10 μs in CG representation. Figure 2 and Figure S4a represent the peptides

127 interacting with BRD at the end of the simulations and show that the peptides form amphipathic
128 beta sheets at the hydrophobic domain of the IMP and present their hydrophilic residues to water.
129 This process can be followed in Fig. 3a and Fig. S5a, which show an increase in the beta sheet
130 content during the simulations, and Fig. 3b and Fig. S5b, where an increase in the area of the
131 interacting surfaces between the peptides and the protein is observed. The peptides are rapidly
132 attracted by the protein surface, and through interactions with BRD, they bury their hydrophobic
133 residues. They form hydrophobic, polar and backbone interactions between the antiparallel or
134 parallel beta strands (Fig. 2). Once at the protein surface, the reorganization of the peptides slowly
135 occurs. The protein surface is 115 nm², and the portion covered by the peptides represents 40 nm².
136 The peptides are also positioned mainly on the hydrophobic part of the protein. They are not
137 always oriented parallel to the helices axis as expected for a beta barrel-like organization.



138 **Figure 2. ADA8 peptide organization on the surface of the membrane protein.** The structures
139 show 20 peptides at the end of the CG simulations when the protein (in yellow) is alone (a) or
140 covered by DPC (c). The protein surrounded by DPC is shown (b), and this structure was used as a
141 starting point before the addition of the peptides (c).

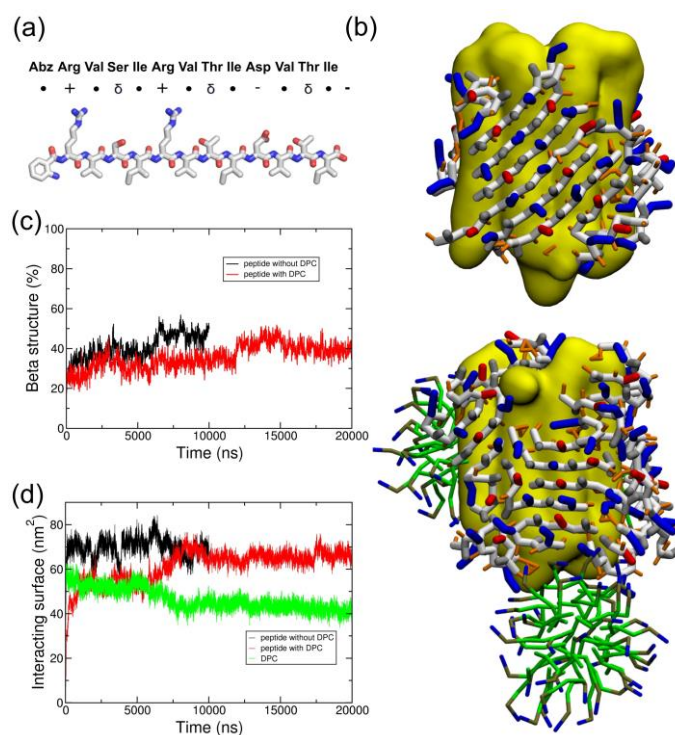
142 Figure 2c shows that when DPC is present at the surface of the protein, the peptide is able to
143 go to the protein surface and form beta sheet structures similar to the situation without DPC.
144 Furthermore, as the peptide is located on the transmembrane domain of BRD, it displaces DPC
145 molecules from the hydrophobic core of the protein (Fig. 2c). DPC molecules are still in interaction
146 with BRD, notably on one of the apical regions where it can interact with two tyrosines and one
147 phenylalanine residue (data not shown). As for the system without DPC, Figure 3 depicts the beta
148 structure (Fig.3a and Fig. S5a) and the surface of the interaction between the peptides and the
149 protein (Fig.3b and Fig. S5b) that are relatively stable along the simulations. To further assess the
150 stability of the interactions and beta structure formed, the structures represented on Fig. 2a and 2c
151 have been transformed to an atomistic resolution and further simulated for 100 ns. These
152 simulations show that the beta sheets formed in CG correspond to stable beta sheets in AT that
153 keep their interactions at the protein surface (see Supplementary Fig. S6).



154 Figure 3. Secondary structure evolution (a) and surface of the interaction (b) of the peptide ADA8 in
 155 the presence of a membrane protein with (red lines) and without (black lines) DPC. The surface of
 156 the interaction between DPC and the membrane protein in the presence of the ADA8 peptide is
 157 green.

158 2.2. Coarse grained simulation of the designed ABZ12 peptide in the presence of a membrane protein

159 To test if this behavior could be extended to similar beta amphipathic peptides, we designed a
 160 peptide called ABZ12 (Fig. 4a). To favor a β conformation, it is composed of residues most
 161 frequently found in β structures, such as Arg, Val, Ile or Thr [22,23]. A size of 12 amino acids is also
 162 compatible with the width of membrane bilayers and is usually observed for membrane proteins
 163 with a beta barrel fold [24,25]. Hydrophobic amino acids (Val and Ile) alternate with hydrophilic
 164 residues (Arg, Thr, and Ser) to generate amphipathy and promote the formation of beta strands [4].
 165 Positive charges in the N-terminal part combined with negative charges at the C-terminal part
 166 should allow an antiparallel arrangement while keeping a global neutrality. A fluorescent N-
 167 terminal cap is added in the form of an aminobenzoyl group for experimental purposes. ATR-
 168 infrared spectroscopy assays of the peptide (see Supplementary Fig. S3) shows a peak at
 169 approximately 1630 cm⁻¹, characteristic of β -sheet conformations. According to what was carried
 170 out for ADA8, CG simulations of the system IMP/ABZ12 in the presence or absence of DPC
 171 molecules were calculated. As shown on Fig. 4b, the same molecular picture is obtained; ABZ12
 172 forms a beta belt around the membrane protein and displaces detergent molecules when they are
 173 present, suggesting a “peptergent-like” behavior. Actually, the detergents moved to more apical
 174 regions of the protein in the presence of the peptides. The beta structure of the peptides stay stable
 175 along the simulations (Fig.4c) and the contact surface between DPC and the protein decreased by at
 176 least 10 nm² (Fig. 4d). For the ABZ12 peptide, formation of DPC micelles can be observed.



177 Figure 4. ABZ12 peptide structure and organization on the surface of the membrane protein. (a)
 178 Representation of the ABZ12 peptide. •, δ, + and - represent hydrophobic, polar, positively and
 179 negatively charged residues, respectively. (b) The structures show 20 peptides at the end of the CG
 180 simulation when the protein (in yellow) is alone or covered by DPC. (c) Secondary structure
 181 evolution and (d) surface of the interaction of the peptide ABZ12 in the presence of a membrane
 182 protein with (red lines) and without (black lines) DPC. The surface of the interaction between DPC
 183 and the membrane protein in the presence of the ABZ12 peptide is in green.

184 3. Discussion

185 In this study, we have analyzed the molecular behavior of ADA8, a well described peptergent,
 186 for the solubilization and stabilization of IMPs through the formation of amphipathic beta barrel
 187 structures by molecular dynamic simulations. The peptide self-assembles into beta structures in
 188 water and is able to interact with membrane proteins, in agreement with the experimental data
 189 previously published [13]. In water, the peptide forms amphipathic beta sheets that look like β-
 190 barrel for the AT representation or a 'sandwich' like β-sheets. It is worth noting that the peptides
 191 were successfully simulated in atomistic and coarse grained representations, validating the CG
 192 approach for such amphipathic peptides. The validation of the CG approach was assessed by using
 193 reverse transformations: hence, AT simulations carried out after reverse transformation showed
 194 that the beta sheets formed in CG were still stable.

195 When a membrane protein is present, the peptide steadily forms a beta sheet structure at the
 196 protein surface and is able to displace DPC surfactants. Tao *et al.* proposed a model for the
 197 organization of the peptides around an IMP [9]. The peptides were thought to generate a beta-
 198 barrel belt around the hydrophobic helical domain that could help stabilize purified membrane
 199 proteins [13]. The MD approaches developed in our study rather agree this view and provide
 200 further molecular details for the replacement of detergent molecules around the protein. Although
 201 a complete belt was not obtained during the course of the simulations, the system tended to move
 202 toward this configuration.

203 In their work, Tao *et al.* also asked how IMPs are stabilized by beta strand peptides that can
 204 assemble into beta aggregated structures in solution [13]. Our calculations suggest that beta sheet
 205 formation is favored in water, suggesting a strong peptide-peptide interaction. In the presence of
 206 membrane proteins, even those solubilized with surfactants, the ADA8 peptide could also form
 207 beta sheets at the protein surface. As the peptide-peptide interaction is stronger than that of

208 surfactants, the former appears to steadily displace surfactants from the protein hydrophobic
209 surface. Since Tao *et al.* showed that their model membrane protein retains its activity, we assumed
210 that the IMP structure is not restrained by the beta sheet structure. Our calculations further suggest
211 that the belt formed around the membrane protein is not 'perfect'. The beta strand can be parallel or
212 antiparallel and beta sheets perpendicular to the protein α helices are observed.

213 Our MD approach could be used to select and design peptides with 'peptergency' properties,
214 i.e. amphiphilic peptides with β sheet structure propensity and the ability to form a β belt-like
215 structure around an IMP in the presence or absence of detergent molecules. As an example, we
216 have designed ABZ12 peptide with a β conformation. As for ADA8 and as expected, this peptide is
217 able to surround the membrane protein and displace the surfactant molecules to the more apical
218 region of the IMP. Preliminary results of FRET assays with ABZ12 show fluorescence energy
219 transfer between the IMP and the aminobenzoic acid group of ABZ12 (data not shown), suggesting
220 a direct interaction between ABZ12 and the protein. Future experimental investigations of the
221 ability of ABZ12 to solubilize membrane proteins should help to confirm its 'peptergency' potential.

222 In conclusion, our MD approach using atomistic and coarse grained representations suggests
223 that one possible mechanism for membrane proteins to be solubilized by β amphipathic self-
224 assembling peptides is the formation of a belt-like structure around the IMP. This belt is not a
225 perfect β barrel, modulating the view that was suggested previously [13]. To our best knowledge,
226 this is the first molecular mechanism proposed for "peptergency".

227 4. Materials and Methods

228 4.1. Peptide synthesis

229 The ABZ12 peptide was synthesized by conventional solid phase peptide synthesis using Fmoc
230 for transient NH₂-terminal protection and was characterized using mass spectrometry. The peptide
231 was lyophilized and resolubilized in DMSO at a final concentration of 10% (w/v) peptide as a stock
232 solution. Before mixing with water, the peptide solution in DMSO was first diluted to 0.5% to avoid
233 insolubility.

234 4.2. FTIR experiments

235 The infrared spectra were measured using a Bruker Equinox 55 spectrometer (Karlsruhe,
236 Germany) equipped with a liquid nitrogen-cooled DTGS detector. The spectra were recorded from
237 4,000 to 750 cm⁻¹ in ATR mode after 1,024 scans at 4 cm⁻¹ resolution and at a two-level zero filling.
238 During the data acquisition, the spectrometer was continuously purged with filtered dried nitrogen.
239 For sample measurement, the peptide solubilized in DMSO was deposited on a germanium plate, and
240 DMSO was evaporated under the N₂ flux for approximately 5 hours. Reference spectra of the
241 germanium plate were automatically recorded and subtracted from the sample spectrum. The
242 resulting spectrum was then smoothed using the Savitzky-Golay algorithm available in the OPUS
243 software.

244 4.3. Systems studied

245 Two peptides were studied by molecular dynamic (MD) simulations; their properties are
246 depicted in Fig. 1 and S2. The ADA8 peptide is described in Tao *et al.* [13]; it contains two non-natural
247 2-aminodecanoic acids (ADA) and is acetylated at the N-terminus and amidated at the C-terminus
248 (Fig. 1b) [13]. The simulated peptide was not N-methylated. This peptide is barely soluble in aqueous
249 solutions and in their study, Tao *et al.* added N-methyl substituents to increase its solubility [13]. The
250 ABZ12 peptide was designed for this study; it is capped at the N-terminus by an aminobenzoic acid
251 and is free at the C-terminus. The peptides have been modeled in an extended conformation based on
252 experimental evidence. The force field Gromos96 54a7 (G54a7) [26] was used during this study. The
253 ABZ topology came from a study by Song *et al.* in 2010 [27], and the ADA topology was derived from
254 the ILE amino acid. The SPC model [28] was used to simulate water. The MARTINI force field [17,29]
255 has been used for coarse grained (CG) simulations. The ABZ residue was replaced by a PHE residue

256 during the coarse grained simulations. The membrane protein used was bacteriorhodopsin (PDBID:
257 1PY6), and its tertiary structure has been maintained with the SAHBNET network [30].

258 4.4. Atomistic molecular dynamic simulations

259 Simulations were performed with the G54a7 force field [26]. All the systems studied (see
260 Supplementary Table S1) were first minimized by steepest descent for 5,000 steps. Then, a 1 ns
261 simulation with the peptides under position restraints was run before the production simulations
262 were performed. Periodic boundary conditions (PBC) were used with a 2 fs time step. All the systems
263 were solvated with SPC water [28] and Na⁺ ions were then added to neutralize the systems. The
264 dynamics were carried out under NPT conditions (298 K and 1 bar). The temperature was maintained
265 using the v-rescale method [31] with $\tau_T = 0.1$ ps, and an isotropic pressure was maintained using the
266 Parrinello-Rahman barostat [32] with a compressibility of 4.5×10^5 (1/bar) and $\tau_P = 5$ ps. The
267 nonbonded interactions were evaluated using a twin-range method. Interactions within the short-
268 range cutoff of 0.8 nm were calculated every step. Interactions within the long-range cutoff of 1.4 nm
269 were recalculated every ten steps, together with the pair list. To correct for the truncation of
270 electrostatic interactions beyond the long-range cutoff, a reaction-field correction was applied using a
271 value of 61 for the relative dielectric permittivity [33]. Bond lengths were maintained with the LINCS
272 algorithm [34]. Trajectories were performed and analyzed with GROMACS 4.5.4 tools as well as with
273 homemade scripts and software. MDAnalysis was also used [35]. The 3D structures were analyzed
274 with both the PyMOL [36] and VMD [37] softwares. The secondary structures were computed with
275 STRIDE [38].

276 4.5. Coarse grained molecular dynamic simulations

277 The peptide models and the BRD protein were converted to a CG representation suitable for the
278 MARTINI force field [17] with the martinize script [39]. Parameters have been developed for the ADA
279 residue from the LEU parameters and atomistic simulations and were added to the martinize script
280 (topologies can be found in supplementary files). No secondary structure were assigned to the
281 peptides through dihedrals and protections of the N- and C-termini were taken into account by
282 setting the first and last BB beads to the P5 type. The coarse grained peptides were placed in a
283 simulation box with water (see Supplementary Table S1). A total of 5,000 steps of steepest-descent
284 energy minimization were performed to remove any steric clashes, and production simulations were
285 run. Temperature and pressure were set at 298 K and 1 bar using the weak coupling Berendsen
286 algorithm [40] with $\tau_T = 1$ ps and $\tau_P = 1$ ps. Pressure was coupled isotropically. Non-bonded
287 interactions were computed up to 1.2 nm with the shift method. Electrostatic interactions were treated
288 with $\epsilon = 15$. The compressibility was 3×10^4 (1/bar). Coarse grained simulations were carried out using
289 Gromacs 4.5.4. [41]

290 To compare the structure evolution between AT and CG, we had to compute a parameter
291 representing the beta structure in CG. Hence, as the backbone is only represented by one bead in CG,
292 it is not possible to compute the phi/psi angles. A dihedral angle greater than 100° and the proximity
293 of two other bonded backbone beads within 6 Å are used to consider a bead to be part of a beta sheet
294 structure. These values have been taken from atomistic simulations and allow for the calculation of
295 the beta structure content with enough precision (see Fig. 1b). The interacting surface between
296 peptides or DPC with the BRD protein has been computed by using the gromacs sasa tool with a
297 probe radius of 0.256 nm which correspond to the radius of the martini particles. The interacting
298 surface correspond to $(SASA_{\text{prot}} + SASA_{\text{pep}} - SASA_{\text{prot+pep}})/2$.

299 Backwards is used for the reverse transformation from a coarse grained to an atomistic
300 representation. The ADA8 peptide is first transformed to a version of the peptide with neutral
301 termini and without the N- and C- terminal protections. The missing atoms are then added with an
302 in house script. A mapping file has been created for the ADA residue.

303 **Supplementary Materials:** Supplementary materials can be found at www.mdpi.com/link.

304 **Acknowledgments:** We would like to thank the FNRS (PDR grant T.1003.14, CDR grants J.0086.18 and
305 J.0114.18), the Belgian Program on Interuniversity Attraction Poles initiated by the Federal Office for Scientific,
306 Technical and Cultural Affairs (IAP P7/44 iPros), and the University of Liège (Action de Recherche Concertée-
307 Project FIELD) for financial support. MD and LL are Senior Research Associates for the Fonds National de la
308 Recherche Scientifique (FRS-FNRS). JMC and MNN were supported by the ARC FIELD project. Partial
309 computational resources of the lab were provided by the “Consortium des Équipements de Calcul Intensif”
310 (CECI) funded by the F.R.S.-FNRS under Grant No. 2.5020.11 and the HPC-Regional Center ROMEO
311 (<https://romeo.univ-reims.fr>) of the University of Reims Champagne-Ardenne (France) for providing CPU
312 time.

313 **Author Contributions:** J-M.C. and L.L. designed the calculations and experiments, JMC performed all
314 calculations and analyses; JMC and LL drafted the manuscript and figures. All authors reviewed the
315 manuscript. A.D., P.M. and P.S. designed the peptide. Infrared spectroscopy was carried out by M.N.N., and
316 the peptide synthesis was carried out by V.S.

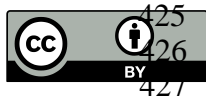
317 **Conflicts of Interest:** "The authors declare no conflict of interest."

318 References

- 319 1. Lakshmanan, A.; Zhang, S.; Hauser, C. A. E. Short self-assembling peptides as building blocks for
320 modern nanodevices. *Trends Biotechnol.* **2012**, *30*, 155–65, doi:10.1016/j.tibtech.2011.11.001.
- 321 2. Mandal, D.; Nasrolahi Shirazi, A.; Parang, K. Self-assembly of peptides to nanostructures. *Org. Biomol.*
322 *Chem.* **2014**, *12*, 3544–61, doi:10.1039/c4ob00447g.
- 323 3. Zhang, S.; Marini, D. M.; Hwang, W.; Santoso, S. Design of nanostructured biological materials through
324 self-assembly of peptides and proteins. *Curr. Opin. Chem. Biol.* **2002**, *6*, 865–71.
- 325 4. Xiong, H.; Buckwalter, B. L.; Shieh, H. M.; Hecht, M. H. Periodicity of polar and nonpolar amino acids is
326 the major determinant of secondary structure in self-assembling oligomeric peptides. *Proc. Natl. Acad. Sci.*
327 *U. S. A.* **1995**, *92*, 6349–53.
- 328 5. Zhang, Q.; Tao, H.; Hong, W.-X. New amphiphiles for membrane protein structural biology. *Methods*
329 **2011**, *55*, 318–23, doi:10.1016/j.ymeth.2011.09.015.
- 330 6. Schafmeister, C. E.; Miercke, L. J.; Stroud, R. M. Structure at 2.5 Å of a designed peptide that maintains
331 solubility of membrane proteins. *Science* **1993**, *262*, 734–8.
- 332 7. McGregor, C.-L.; Chen, L.; Pomroy, N. C.; Hwang, P.; Go, S.; Chakrabartty, A.; Privé, G. G. Lipopeptide
333 detergents designed for the structural study of membrane proteins. *Nat. Biotechnol.* **2003**, *21*, 171–6,
334 doi:10.1038/nbt776.
- 335 8. Wang, X.; Huang, G.; Yu, D.; Ge, B.; Wang, J.; Xu, F.; Huang, F.; Xu, H.; Lu, J. R. Solubilization and
336 stabilization of isolated photosystem I complex with lipopeptide detergents. *PLoS One* **2013**, *8*, e76256,
337 doi:10.1371/journal.pone.0076256.
- 338 9. Ho, D. N.; Pomroy, N. C.; Cuesta-Seijo, J. A.; Privé, G. G. Crystal structure of a self-assembling
339 lipopeptide detergent at 1.20 Å. *Proc. Natl. Acad. Sci. U. S. A.* **2008**, *105*, 12861–6,
340 doi:10.1073/pnas.0801941105.
- 341 10. Kiley, P.; Zhao, X.; Vaughn, M.; Baldo, M. a; Bruce, B. D.; Zhang, S. Self-assembling peptide detergents
342 stabilize isolated photosystem I on a dry surface for an extended time. *PLoS Biol.* **2005**, *3*, e230,
343 doi:10.1371/journal.pbio.0030230.
- 344 11. Zhao, X.; Nagai, Y.; Reeves, P. J.; Kiley, P.; Khorana, H. G.; Zhang, S. Designer short peptide surfactants
345 stabilize G protein-coupled receptor bovine rhodopsin. *Proc. Natl. Acad. Sci. U. S. A.* **2006**, *103*, 17707–12,
346 doi:10.1073/pnas.0607167103.
- 347 12. Corin, K.; Baaske, P.; Ravel, D. B.; Song, J.; Brown, E.; Wang, X.; Wienken, C. J.; Jerabek-Willemsen, M.;
348 Duhr, S.; Luo, Y.; Braun, D.; Zhang, S. Designer lipid-like peptides: A class of detergents for studying
349 functional olfactory receptors using commercial cell-free systems. *PLoS One* **2011**, *6*, e25067,
350 doi:10.1371/journal.pone.0025067.
- 351 13. Tao, H.; Lee, S. C.; Moeller, A.; Roy, R. S.; Siu, F. Y.; Zimmermann, J.; Stevens, R. C.; Potter, C. S.;
352 Carragher, B.; Zhang, Q. Engineered nanostructured β -sheet peptides protect membrane proteins. *Nat.*
353 *Methods* **2013**, *10*, 759–761, doi:10.1038/nmeth.2533.
- 354 14. Carpenter, E. P.; Beis, K.; Cameron, A. D.; Iwata, S. Overcoming the challenges of membrane protein
355 crystallography. *Curr. Opin. Struct. Biol.* **2008**, *18*, 581–6, doi:10.1016/j.sbi.2008.07.001.
- 356 15. Ge, B.; Yang, F.; Yu, D.; Liu, S.; Xu, H. Designer amphiphilic short peptides enhance thermal stability of
357 isolated photosystem-I. *PLoS One* **2010**, *5*, e10233, doi:10.1371/journal.pone.0010233.
- 358 16. Moeller, A.; Lee, S. C.; Tao, H.; Speir, J. A.; Chang, G.; Urbatsch, I. L.; Potter, C. S.; Carragher, B.; Zhang,
359 Q. Distinct conformational spectrum of homologous multidrug ABC transporters. *Structure* **2015**, *23*, 450–
360 60, doi:10.1016/j.str.2014.12.013.
- 361 17. Monticelli, L.; Kandasamy, S. K.; Periolo, X.; Larson, R. G.; Tieleman, D. P.; Marrink, S. The MARTINI
362 Coarse-Grained Force Field: Extension to Proteins. *J. Chem. Theory Comput.* **2008**, *4*, 819–834,
363 doi:10.1021/ct700324x.
- 364 18. Hung, A.; Yarovsky, I. Inhibition of peptide aggregation by lipids: insights from coarse-grained
365 molecular simulations. *J. Mol. Graph. Model.* **2011**, *29*, 597–607, doi:10.1016/j.jm gm.2010.11.001.
- 366 19. Sørensen, J.; Periolo, X.; Skeby, K. K.; Marrink, S.-J.; Schiøtt, B. Protofibrillar Assembly Toward the
367 Formation of Amyloid Fibrils. *J. Phys. Chem. Lett.* **2011**, *2*, 2385–2390, doi:10.1021/jz2010094.

- 368 20. Seo, M.; Rauscher, S.; Pomès, R.; Tieleman, D. P. Improving Internal Peptide Dynamics in the Coarse-
369 Grained MARTINI Model: Toward Large-Scale Simulations of Amyloid- and Elastin-like Peptides. *J.*
370 *Chem. Theory Comput.* **2012**, *8*, 1774–1785, doi:10.1021/ct200876v.
- 371 21. Marrink, S. J.; Tieleman, D. P. Perspective on the Martini model. *Chem. Soc. Rev.* **2013**, *42*, 6801–22,
372 doi:10.1039/c3cs60093a.
- 373 22. Bhattacharjee, N.; Biswas, P. Position-specific propensities of amino acids in the β -strand. *BMC Struct.*
374 *Biol.* **2010**, *10*, 29, doi:10.1186/1472-6807-10-29.
- 375 23. Malkov, S. N.; Zivković, M. V.; Beljanski, M. V.; Hall, M. B.; Zarić, S. D. A reexamination of the
376 propensities of amino acids towards a particular secondary structure: classification of amino acids based
377 on their chemical structure. *J. Mol. Model.* **2008**, *14*, 769–75, doi:10.1007/s00894-008-0313-0.
- 378 24. Wimley, W. C. The versatile beta-barrel membrane protein. *Curr. Opin. Struct. Biol.* **2003**, *13*, 404–11.
- 379 25. Jackups, R.; Liang, J. Interstrand pairing patterns in beta-barrel membrane proteins: the positive-outside
380 rule, aromatic rescue, and strand registration prediction. *J. Mol. Biol.* **2005**, *354*, 979–93,
381 doi:10.1016/j.jmb.2005.09.094.
- 382 26. Schmid, N.; Eichenberger, A. P.; Choutko, A.; Riniker, S.; Winger, M.; Mark, A. E.; van Gunsteren, W. F.
383 Definition and testing of the GROMOS force-field versions 54A7 and 54B7. *Eur. Biophys. J.* **2011**, *40*, 843–
384 56, doi:10.1007/s00249-011-0700-9.
- 385 27. Song, B.; Kibler, P.; Malde, A.; Kodukula, K.; Galande, A. K. Design of short linear peptides that show
386 hydrogen bonding constraints in water. *J. Am. Chem. Soc.* **2010**, *132*, 4508–9, doi:10.1021/ja905341p.
- 387 28. Hermans, J.; Berendsen, H. J. C.; Van Gunsteren, W. F.; Postma, J. P. M. A consistent empirical potential
388 for water-protein interactions. *Biopolymers* **1984**, *23*, 1513–1518, doi:10.1002/bip.360230807.
- 389 29. Marrink, S. J.; Risselada, H. J.; Yefimov, S.; Tieleman, D. P.; de Vries, A. H. The MARTINI force field:
390 coarse grained model for biomolecular simulations. *J. Phys. Chem. B* **2007**, *111*, 7812–24,
391 doi:10.1021/jp071097f.
- 392 30. Dony, N.; Crowet, J. M.; Joris, B.; Basseur, R.; Lins, L. SAHBNET, an Accessible Surface-Based Elastic
393 Network: An Application to Membrane Protein. *Int. J. Mol. Sci.* **2013**, *14*, 11510–26,
394 doi:10.3390/ijms140611510.
- 395 31. Bussi, G.; Donadio, D.; Parrinello, M. Canonical sampling through velocity rescaling. *J. Chem. Phys.* **2007**,
396 *126*, 014101, doi:10.1063/1.2408420.
- 397 32. Parrinello, M. Polymorphic transitions in single crystals: A new molecular dynamics method. *J. Appl.*
398 *Phys.* **1981**, *52*, 7182, doi:10.1063/1.328693.
- 399 1.
- 400 33. Heinz, T. N.; van Gunsteren, W. F.; Hunenberger, P. H. Comparison of four methods to compute the
401 dielectric permittivity of liquids from molecular dynamics simulations. *J. Chem. Phys.* **2001**, *115*, 1125–
402 1136.
- 403 34. Hess, B.; Bekker, H.; Berendsen, H. J. C.; Fraaije, J. G. E. M. LINCS: A linear constraint solver for
404 molecular simulations. *J. Comput. Chem.* **1997**, *18*, 1463–1472, doi:10.1002/(SICI)1096-
405 987X(199709)18:12<1463::AID-JCC4>3.0.CO;2-H.
- 406 35. Michaud-Agrawal, N.; Denning, E. J.; Woolf, T. B.; Beckstein, O. MDAAnalysis: a toolkit for the analysis of
407 molecular dynamics simulations. *J. Comput. Chem.* **2011**, *32*, 2319–27, doi:10.1002/jcc.21787.
- 408 36. Schrödinger, L. The PyMOL Molecular Graphics System, Version 1.3 2010.
- 409 37. Humphrey, W.; Dalke, A.; Schulten, K. VMD: visual molecular dynamics. *J. Mol. Graph.* **1996**, *14*, 33–8,
410 27–8.
- 411 38. Frishman, D.; Argos, P. Incorporation of non-local interactions in protein secondary structure prediction
412 from the amino acid sequence. *Protein Eng.* **1996**, *9*, 133–42.
- 413 39. de Jong, D. H.; Singh, G.; Bennett, W. F. D.; Arnarez, C.; Wassenaar, T. A.; Schäfer, L. V.; Periole, X.;
414 Tieleman, D. P.; Marrink, S. J. Improved Parameters for the Martini Coarse-Grained Protein Force Field.
415 *J. Chem. Theory Comput.* **2013**, *9*, 687–697, doi:10.1021/ct300646g.
- 416 40. Berendsen, H. J. C.; Postma, J. P. M.; van Gunsteren, W. F.; DiNola, a; Haak, J. R. Molecular dynamics
417 with coupling to an external bath. *J. Chem. Phys.* **1984**, *81*, 3684–3690, doi:10.1063/1.448118.
- 418 41. Hess, B.; Kutzner, C.; van der Spoel, D.; Lindahl, E. GROMACS 4: Algorithms for Highly Efficient, Load-
419 Balanced, and Scalable Molecular Simulation. *J. Chem. Theory Comput.* **2008**, *4*, 435–447,
420 doi:10.1021/ct700301q.

- 421 42. Wassenaar, T.A.; Pluhackova, K.; Böckmann, R. A.; Marrink, S. J.; Tieleman, D. P. Going backward: A
422 flexible geometric approach to reverse transformation from coarse grained to atomistic models. *J. Chem.*
423 *Theory Comput.* **2013**, *10*, 676-690, doi:10.1021/ct400617g.
424



425 © 2017 by the authors. Submitted for possible open access publication under the
426 terms and conditions of the Creative Commons Attribution (CC BY) license
427 (<http://creativecommons.org/licenses/by/4.0/>).